Plant Archives Volume 20 No. 1, 2020 pp. 1196-1200 **e-ISSN:2581-6063 (online), ISSN:0972-5210**

GREEN SYNTHESIS, CHARACTERIZATION AND ANTIBACTERIAL ACTIVITY OF IRON OXIDE NANOPARTICLES

Ritu Hooda and Minakshi Sharma*

Department of Zoology, Maharshi Dayanand University, Rohtak (Haryana), India.

Abstract

A green approach to synthesize nanoparticles has been used recently to evade the toxicity of reducing reagents used. We have synthesized iron oxide nanoparticles (Fe_2O_3NPs) via green route using leaf extract of *Citrus* (Lemon) and characterized by UV–Visible spectroscopy, Transmission electron microscopy, Energy dispersive X-ray diffraction, X-ray diffractometer, Fourier transform infrared spectroscopy and Zeta analysis. The Fe_2O_3NPs also showed an interesting antibacterial activity against gram-positive (*Bacillus subtilis*) and gram-negative (*Klebsiella pneumonia*), human gut pathogenic bacteria at microgram concentrations.

Key words : Iron oxide nanoparticles, green nanotechnology, and antibacterial activity.

Introduction

Large scale urbanization and industrialization have contributed to today's environmental calamities principally in aquatic domain. Nanoparticle (NPs) synthesis is one of the most emerging processes to cope with various organic and inorganic toxic pollutants (Tahir *et al.,* 2016). In recent years, iron nanoparticles (Fe_2O_3NPs) due to their diversified applications are being actively looked into. Fe_2O_3NPs are characterized as active agents against many organic and inorganic pollutants. These iron-based nanoparticles have been reported in different states i.e. zero valent iron (Cai *et al.*, 2014), Fe ball clay (Poguberovic *et al.*, 2016), Fe_2O_3NPs (Salam *et al.*, 2015). Minuscule size, large surface area and high degree of dispersion of NPs make them unique for their catalytic activity. Owing to high magnetic susceptibility and biocompatibility, Fe_2O_3NPs have been magnificently employed in various therapeutics for cancer treatment and radiation oncology (Park *et al.,* 2015). Various distinctive methods have been in practice to manufacture nanoparticles. The methods used for their production fall under chemical, physical and biosynthetic domains. Some of these chemical processes include thermal decomposition (Kandasamy and Maity, 2015), co-precipitation (Xie *et al.,* 2006), sol-gel method (Unsoy *et al.,* 2012), polyol methods (Lemine *et al.,* 2014) and hydrothermal method (Zhang *et al.,* 2012). These conventional methods are not as enticing as they lead to degradation of the ecosystem, exhibit low dispersion rates, are expensive, exhibit low uniformity in dispersion and are inconvenient to work with in scaled-up applications. Contemporary to these methods, green synthesis stands out showcasing the encouraging results and a wide range of flexible effects which include no demand of optimum operating conditions, stable economical perspectives and their hospitable approach to environment. Green synthetic process has already been used to fabricate various metal NPs and nano composites such as silver, palladium, gold NPs, ZnO NPs, Au/TiO2 and Cu/ZnO nanocomposite (Momeni *et al.,* 2016). Over the previous time, it has been recognized that there is an interaction between biomolecules, such as proteins, nucleic acids, lipids and even biological metabolites with nanoparticles due to their nano-size and large surface-to-mass ratio. Of particular importance is the adsorption of proteins on the NPs surface. The formation of NPs-protein complexes is commonly referred to as the NPs-protein corona. A number of consequences of protein adsorption on the NP surface can be speculated. Overall, the NPs-protein corona can influence the biological reactivity of the

***Author for correspondence :** E-mail: sminakshi.2007@rediffmail.com

biomolecules (Casals *et al.*, 2010).

Some Fe_2O_3NPs eventually enter the aquatic systems, raising concerns about toxicity from aqueous exposure. To investigate the effects of exposure to Fe_2O_3NPs both in vivo and vitro, xanthine oxidase (XO) was used in this study. Specifically, we determined the impact of Fe_2O_3NPs on XO when incubated with it. The present study describes herein the green synthesis of Fe_2O_3NPs using leaf extract of *Citrus* (Lemon), their characterization by various physicochemical techniques and its impact on activity of XO and gram positive and negative bacterial growth. This impact of green Fe_2O_3NPs on XO activity, have also been compared with chemically synthesized Fe_2O_3NPs (commercial). The study could also help to further evaluate the long-term impact of Fe_2O_3NPs on enzyme (XO).

Materials and Methods

Chemicals and reagents

Iron (II) oxide nanopowder (<50 nm particle size), iron chloride and ampicillin were from Himedia Laboratories Pvt. Ltd., Mumbai, India. Other chemicals were of analytical reagent grade. Distilled water (DW) was used throughout the study. The culture of *B. subtilis* (MTCC-441) and *K. pneumoniae* (MTCC-2405) were obtained from Institute of Microbial Technology (IMTECH), Chandigarh, India. *P. granatum* leaves were collected from the Herbal garden of Maharshi Dayanand University, Rohtak (Haryana) India.

Synthesis of Fe_2O_3NPs

Fresh leaves of *Citrus* (25g) were washed under running tap water followed by DW and then homogenized in 250 mL DW in a warring blender. The homogenate was kept at 55°C for 30 min and then passed through a Millipore hydrophilic filter (0.22 μm), and then filtered through Whatman no. 1 filter paper three times. The obtained filtrate was chilled at 4°C for further use. To synthesize Fe_2O_3NPs, 15 ml aqueous solution of *Citrus* leaf extract and 85 ml of iron chloride (0.1 mM) solution were mixed in a 250 ml Erlenmeyer flask. The pH of this mixture was adjusted to pH 10.0 and kept under continuous stirring at 55°C. After 4 h of continuous stirring, the mixture/solution showed a color alteration from brown to black, indicating the reduction of pure Fe^{+2} ions and confirming the synthesis of Fe_2O_3NPs (Devatha *et al.*, 2016). The pH of the mixture containing leaf extract was pH 5.6, while after addition of 1 mM iron chloride, pH was reduced to 3.1 indicating formation of Fe_2O_3NPs. After that, the mixture/extract + Fe_2O_3NPs were centrifuged at 5,500 rpm for 15 min and the pellet was redispersed in DW. This process of centrifugation was repeated thrice to ensure better separation of the Fe_2O_3NPs. The purified solution of Fe_2O_3NPs was then dried in oven to obtain its powder. The purified dried powder of Fe_2O_3NPs was then used for characterization.

Characterization of Fe_2O_3NPs

The formation of green Fe_2O_3NPs was confirmed firstly by, UV–visible spectrophotometer (UV-1601, Shimadzu, Japan) against DW as a control and then by FTIR spectroscopy. The FTIR was done in the series of 4000–500 cm^{-1} and at a resolution of 4 cm^{-1} via a Bruker (Germany), Alpha Model. TEM (TECNAI 200 Kv, FEI, USA) was done, which provided the shape and structure of the green Fe_2O_3NPs. The Fe_2O_3NPs in dried form was further analyzed by XRD meter ((PANalyticalX'Pert PRO, Netherlands). The XRD graph was measured, which worked at a voltage of 40 kV, a current of 30 mA with CuKβ radiation and in the range of 20–80 °C (2θ). The steadiness of green Fe_2O_3NPs was measured by Malvern Zetasier Nano Z, UK, device.

Antibacterial assay

Antibacterial activity of synthesized green Fe_2O_3NPs was measured by disc diffusion process, against two pathogenic bacteria *B. subtilis* (MTCC-441) and *K. pneumonia* (MTCC-2405) (Chowdhury *et al.*, 2013). The bacteria were sub-cultured from the pure cultures, at 35 °C on Nutrient broth, at 200 rpm on a rotary shaker. Both strains were poured, spread and swabbed homogeneously on the each plate with sterile cotton swabs. The sterile Whatman no. 1 filter paper discs of 6 mm size were placed on plates. 5 μl of ampicillin (1 mg ml^{-1}) was taken as a positive control, three different concentrations of the Fe_2O_3NPs nanoparticles solution 25 μl, 50 μl and 100 μl, were taken and distilled water (10μl) was taken as negative control, all were poured cautiously on the discs and incubated at 37 °C for 24 h. A clear and transparent zone of inhibition around the discs was showed by the bacteria. Zone of inhibition was measured via a meter ruler, the mean value for each bacterium was measured and articulated in millimeter (Table 1).

Results and Discussion

Characterization of Fe_2O_3NPs

UV-visible spectroscopy is a method to analyze the reduction of precursors has occurred, in the range of 200- 600 nm. The UV Visible spectrum of Fe_2O_3NPs is shown in Fig. 1. There is a strong absorption peak at 400 nm indicating the formation of Fe_2O_3NPs (Rahman *et al.*, 2011). The FTIR spectrum provides the occurrence of different functional groups, responsible for the

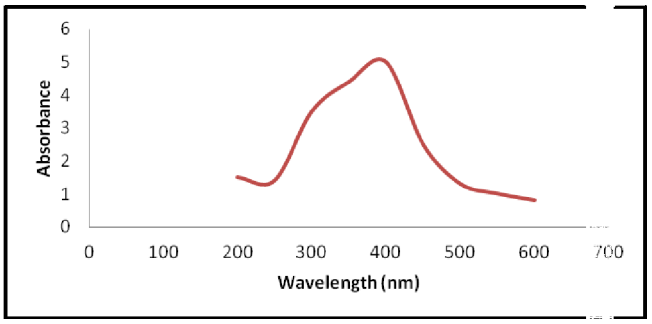

Fig. 1: (a) UV–Vis spectra of Fe_2O_3-NPs synthesized by leaf extract of *Citrus.*

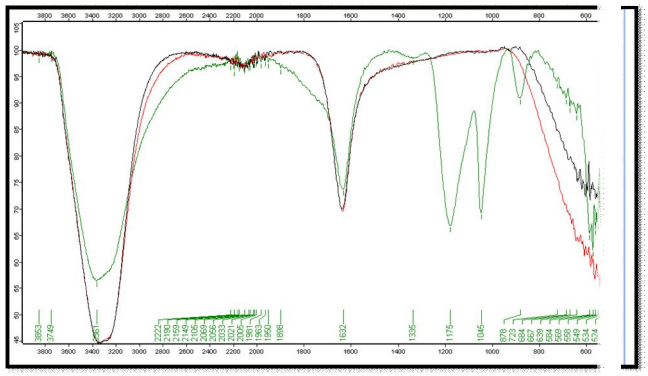

Fig. 2: FTIR spectra of Fe_2O_3-NPs synthesized by leaf extract of *Citrus.*

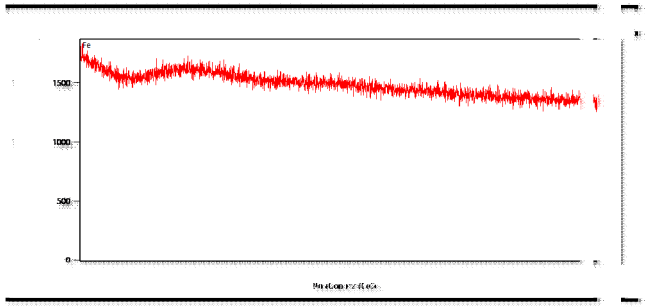

Fig. 3: XRD spectra of Fe_2O_3-NPs synthesized by leaf extract of *Citrus.*

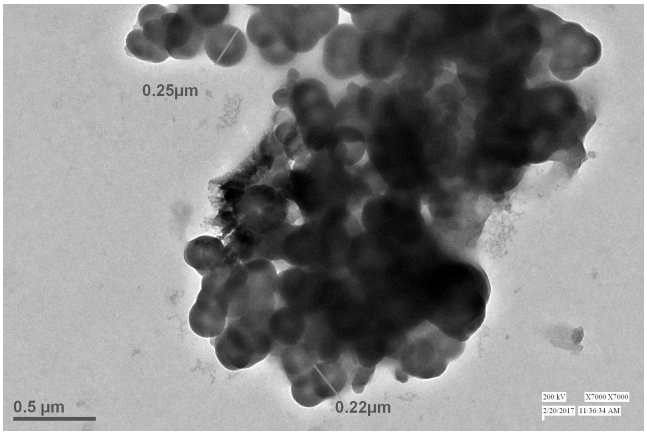

Fig. 4: TEM images of Fe_2O_3-NPs synthesized by leaf extract of *Citrus.*

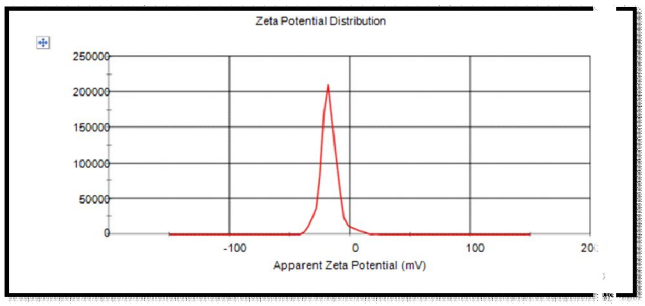

Fig. 5: Zeta analysis of Fe_2O_3-NPs synthesized by leaf extract of *Citrus.*

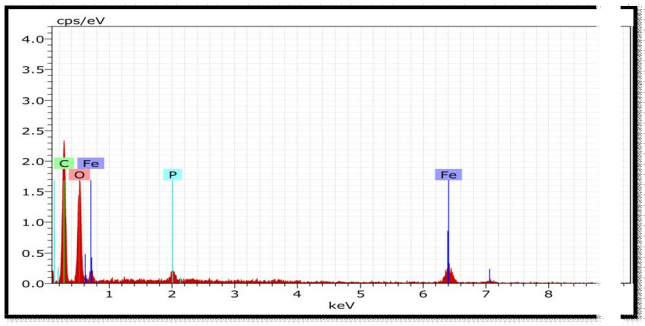

Fig. 6: EDX spectra of Fe_2O_3-NPs synthesized by leaf extract of *Citrus.*

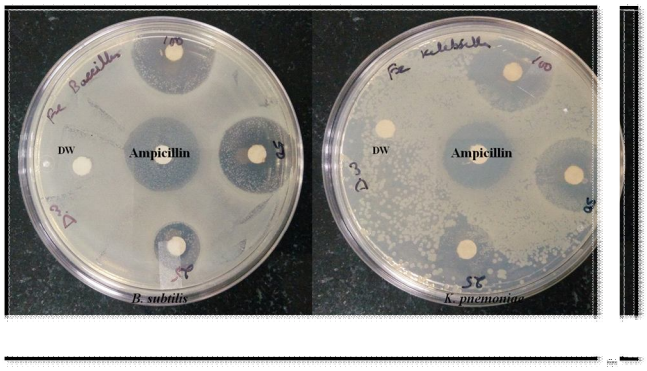

Fig. 7: Bacterial culture showing the inhibition zone around well loaded for different concentrations of green Fe_2O_3NPs (a) *B. subtilis* (b) *K. pneumoniae.*

reduction of Fe^{3+} and synthesis of Fe_2O_3NPs. FTIR analysis of the Fe_2O_3NPs is shown in Fig. 2. The prominent peaks were observed at 3361 cm^{-1}, 1632 cm^{-1}, 1175 cm^{-1}, 1045 cm^{-1}, 878 cm^{-1}. The presence of sharp peak at 3361 cm^{-1} is due to –OH stretching in alcohol and phenolic compounds present in lemon extract. The presence of sharp peak at 1632 cm^{-1}, 1175 cm^{-1}, 1045 cm^{-1} and 878 cm^{-1} corresponds to carbonyl stretching, N-H bend primary amines, C-N stretching of the aromatic amino group and C-O stretching alcohols, ethers respectively (Rahman *et al.*, 2011; Coates, 2006). FTIR spectrum of Fe_2O_3NPs suggested that Fe_2O_3NPs were surrounded by different organic molecules such as terpenoids, alcohols, ketones, aldehydes and carboxylic acid (Raut

Table 1: Zone of inhibition due to Fe_2O_3NPs against gram positive and gram negative bacteria.

Concentration of Fe_2O_3NPs (µg/ml)	Zone of Inhibition (mm)		
	B. subtilis	*K. pneumoniae*	Ampicillin(1 mg/ml) (+ control)
100	26.1± 0.24	21.5±0.36	12.8±0.52
50	24.1±0.37	18.3±0.49	
25	12.8±0.69	11.7±0.53	

et al., 2010).

The crystalline structure of the Fe_2O_3NPs was investigated by X-ray diffraction using X-ray diffractometer (Bruker, D2-Phaser). XRD spectrum was recorded from 10 to 80^0 2θ angles using CuKβ radiation operated at 40kV and 40 mA. XRD patterns of Fe_2O_3NPs are presented in Fig. 3. XRD spectra of Fe_2O_3NPs displayed number of strong peaks 23^0, 33^0, 35^0, 40^0, 53^0, 63^0 which are closely matched with the values of rhombohedral crystalline structure (Fe_2O_3). These results were confirmed by comparing the peak values matched with JCPDS card (card no. 89-2810) (Radhakrishnan *et al.,* 2013).

The TEM images of green Fe_2O_3NPs have shown its structure as electron-dense mostly spherical particles with a diameter in the range of 15 to 80 nm with the average size 40nm shown in Fig. 4. The zeta potential of Fe_2O_3NPs dispersed in water was found to be -17 mV which indicates that the synthesized particles were stable shown in Fig. 5. The EDX spectra recorded from the Fe_2O_3NPs is shown in Fig. 6. The spectrum shows a strong iron signal in the iron region and established the formation of Fe_2O_3NPs (Waseem *et al.,* 2014). Metallic iron nanocrystals generally show typical absorption peak, approximately at 1 and 8 keV, is typical for the absorption of iron oxide nanocrystallites due to Surface Plasmon Resonance. There are weak oxygen, carbon and phosphorous peaks, which may have originated from the biomolecules bound to the surface of the Fe_2O_3NPs.

Antibacterial activity of Fe_2O_3NPs

Fe_2O_3NPs antibacterial activity was assessed against the two human gut pathogenic bacteria *B. subtilis* and *K. pneumonia* by disc diffusion method. The zone of inhibition of bacteria by the effect of Fe_2O_3NPs for different concentrations was shown in Fig. 7. With increase in concentration of Fe_2O_3NPs it was seen that there was an increase in the size of zone of inhibition for both the bacterias tested. The radial diameters of zone of inhibition were measured in millimeter for *B. subtilis* than *K. pneumoniae* and ampicillin, are as shown in Table. 1. It can be said that Fe_2O_3NPs carries more ability to kill the bacterias as compared to ampicillin. Also, they displayed greater antibacterial activity for *B. subtilis* as compared to *K. pneumoniae* and thus, it can be said that Fe_2O_3NPs are more effective against the gram +ve as compared to gram –ve.

Conclusion

Fe_2O_3NPs were prepared by green synthesis using lemon leaf extract and characterized by various physicochemical techniques. Our results showed that green Fe_2O_3NPs are stable, spherical in shape, have average size 40 nm and rhombohedral crystalline structure. The green Fe_2O_3NPs showed a good antibacterial activity against two human gut pathogenic bacterial strains.

Acknowledgement

One of the authors (RH) is grateful to Maharshi Dayanand University, Rohtak for the award of university research scholarship during the tenure of this study.

References

Cai, X., Y. Gao, Q. Sun, Z. Chen and M.R. Megharaj (2014). Naidu, Removal of co-contaminants Cu (II) and nitrate from aqueous solution using kaolin-Fe/Ni nanoparticles. *Chemical Engineering Journal*, **244:** 19–26.

Casals, E., T. Pfaller, A. Duschl, G.J. Oostingh and V. Puntes (2010). Time Evolution of the Nanoparticle Protein Corona. *ACS Nano*, **4:** 3623–3632.

Chowdhury, M.N.K., M.D.H. Beg, M.R. Khan and M.F. Mina (2013). Synthesis of copper nanoparticles and their antimicrobial performances in natural fibres. *Materials Letters*, **98:** 26-29.

Coates, J. (2006). Interpretation of Infrared Spectra. A Practical Approach. Encyclopedia of Analytical Chemistry.

Devatha, C.P, A.K. Thalla and S.Y. Katte (2016). Green synthesis of iron nanoparticles using different leaf extracts for treatment of domestic waste water. *Journal of cleaner production*, **139:**1425-1435.

Kandasamy, G.D.M. (2015). Recent advances in superparamagnetic Iron oxide nanoparticles (SPION) for in vitro and in vivo cancer nanotheranostic. *International journal of pharmaceutics*, **496:** 191-218.

Hassan, H. and B.H. Hameed (2011). Fe–clay as effective heterogeneous Fenton catalyst for the decolorization of Reactive Blue 4. *Chemical Engineering Journal*, **171:** 912–918.

Lemine, O.M., K. Omri, M. Iglesias, V. Velasco, P. Crespo, P. de la Presa and L. El Mira (2014). λ-Fe_2O_3 by sol–gel with large nanoparticles size for magnetic hyperthermia application. *Journal of Alloys and Compounds*, **607:** 125–131.

Momeni, S.S., M. Nasrollahzadeh and A. Rustaiyan (2016). Green synthesis of the Cu/ZnO nanoparticles mediated

by *Euphorbia prolifera* leaf extract and investigation of their catalytic activity. *J. Colloid Interface Sci*., **472:** 173–179.

Park, H.S, J.R. Koduru, K.H. Choo and B. Lee (2015). Activated carbons impregnated with iron oxide nanoparticles for enhanced removal of bisphenol A and natural organic matter. *Journal of Hazardous Materials*, **286:** 315–324.

Poguberovic, S.S., D.M. Krcmar, S.P. Maletic, Z. Konya, D.D.T. Pilipovic, D.V. Kerkez and S.D. Roncevic (2016). Removal of As(III) and Cr(VI) from aqueous solutions using "green" zero valent iron nanoparticles produced by oak, mulberry and cherry leaf extracts. *Ecological Engineering*, **90:** 42–49.

Radhakrishnan, S., K. Krishnamoorthy, C. Sekar, J. Wilson and S.J. Kim (2014). A highly sensitive electrochemical sensor for nitrite detection based on Fe2O3 nanoparticles decorated reduced graphene oxide nanosheets. *Applied Catalysis B: Environmental*, **148:** 22-8.

Rahman, M.M., S.B. Khan, A. Jamal, M. Faisal and A.M. Aisiri (2011). Iron oxide nanoparticles. *Nanomaterials*, **3:** 43-67.

Raut, RW., N.S. Kolekar, J.R. Lakkakula, V.D. Mendhulkar and S.B. Kashid (2010). Extracellular Synthesis of Silver Nanoparticles Using Dried Leaves of *Pongamia pinnata* (L) Pierre. *Nano-Micro Letters*, **2:** 106-113.

Salam, M.A., O. Fageeh, S.A. Al-Thabaiti and A.Y. Obaid (2015). Removal of nitrate ions from aqueous solution using zero-valent iron nanoparticles supported on high surface area nano graphenes. *Journal of Molecular Liquids*, **212:** 708–715.

Tahir, K., S. Nazir, A. Ahmad, B. Li, S.A.A. Shah, A.U. Khan, G. M. Khan, Q.U Khan, Z.U.H. Khan and F.U. Khan (2016). Biodirected synthesis of palladium nanoparticles using Phoenix dactylifera leaves extract and their size dependent biomedical and catalytic applications. *RSC Adv*., **6:** 85903.

Unsoy, G.S. R. Yalcin, Khodadust and G.G.U. Gunduz (2012). Synthesis optimization and characterization of chitosan coated iron oxide nanoparticles produced for biomedical applications. J. *Nanopart Res*., **14:** 964.

Waseem, M., S. Munsif and U. Rashid (2014). Physical properties of α-Fe_2O_3 nanoparticles fabricated by modified hydrolysis technique. *Applied Nano-science*, **4(5):** 643-648.

Xie, J., S. Peng, N. Brower, N. Pourmand, S.X.Wang and S. Sun (2006). One-pot synthesis of monodisperse iron oxide nanoparticles for potential biomedical applications. *Pure Appl. Chem*., **78:** 1003–1014.

Zhang, B.Z. Tu, F. Zhao and J. Wang (2013). Superparamagnetic iron oxide nanoparticles prepared by using an improved polyol method. *Applied Surface Science*, **266:** 375–379.